AN EFFICIENT METHOD FOR CALCULATING RMS VON MISES STRESS IN A RANDOM VIBRATION ENVIRONMENT

Daniel J. Segalman, Clay W. G. Fulcher, Garth M. Reese, and Richard V. Field, Jr.

Structural Dynamics and Vibration Control Department
Sandia National Laboratories
P.O. Box 5800
Albuquerque, New Mexico 87185-0439

ABSTRACT. An efficient method is presented for calculation of RMS von Mises stresses from stress component transfer functions and the Fourier representation of random input forces. An efficient implementation of the method calculates the RMS stresses directly from the linear stress and displacement modes. The key relation presented is one suggested in past literature, but does not appear to have been previously exploited in this manner.

NOMENCLATURE

$f_i^j(t)$	input force time history in direction i at location j
$\hat{f}$	frequency-domain representation of $f(t)$
$h(t)$	impulse response function matrix
$p(t)$	von Mises stress time history
$D_j(\omega)$	frequency dependence in stress transfer functions
H	transfer function matrix
N_ω	number of frequency points
N_F	number of input force locations
PSD	power spectral density
RMS	root mean square
S_F	input force cross spectral density matrix
s_F	input force autospectral density
$\sigma(t)$	stress vector (6 x 1)
φ_{aj}	displacement eigenvector for mode i at d.o.f. a
$\Psi_{\sigma_T^i}$	stress vector for mode i, evaluated at node b
$(\ )^T$	matrix transpose
$\langle\ \rangle$	time average
$E[\ ]$	expected value operator
$\bar{(\ )}$	complex conjugate
$(\ )^\dagger$	Hermitian (complex conjugate transpose)

1. INTRODUCTION

The primary purpose of finite element stress analysis is to estimate the reliability of engineering designs. In structural applications, the von Mises stress due to a given load is often used as the metric for evaluating design margins. For deterministic loads, both static and dynamic, the calculation of von Mises stress is straightforward [1]. For random load environments typically defined in terms of power spectral densities, the linear theory normally applied to compute RMS acceleration, displacement, or stress tensor responses cannot be applied directly to calculate the RMS von Mises stress, a nonlinear function of the linear stress components. Although, what is ultimately sought is *not* the frequency distribution or time history of the von Mises stress but it's RMS value, the probability distribution of von Mises stress is not Gaussian, nor is it centered about zero as are the stress components. Therefore, the form of the von Mises probability distribution must be determined and the parameters of that distribution must be found. Due to space constraints, determination of the von Mises probability distribution will be the subject of a later paper.

The most direct method of calculating von Mises stress from frequency data requires computation of a long time series of linear stress components. The stress invariants can be computed at each time step and an RMS value determined through time integration. This process is of order $N_\omega^2 \log N_\omega$ for each output location. This expensive computational procedure makes broad surveying for von Mises stress impractical. Computationally simpler methods, such as Miles' relation [2], involve significant approximations that can be nonconservative [3].

A new, computationally efficient process for computing the RMS values of von Mises stress is introduced. The new method enables the analyst to perform surveys of von Mises stress routinely, allowing a thorough investigation into the reliability of an engineering design. This method accounts for the full frequency response of the structure.

2. THE PROBLEM

In a typical random vibration test, a structure is attached to a single input load source, such as a shaker table, and subjected to a vibratory load characterized by a specified power spectral density (PSD) of the input acceleration. To illustrate the problem, a finite element model of an aluminum cylinder, subjected to transverse random vibration at the base, was created using shell elements. Figs. 1 and 2 show the cylinder model and the input acceleration PSD applied at the base, respectively. Current standard procedure is to

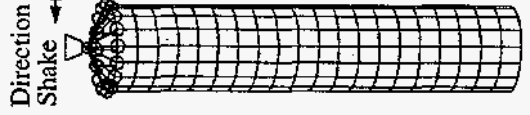

Figure 1: Cylinder FEM.

DISCLAIMER

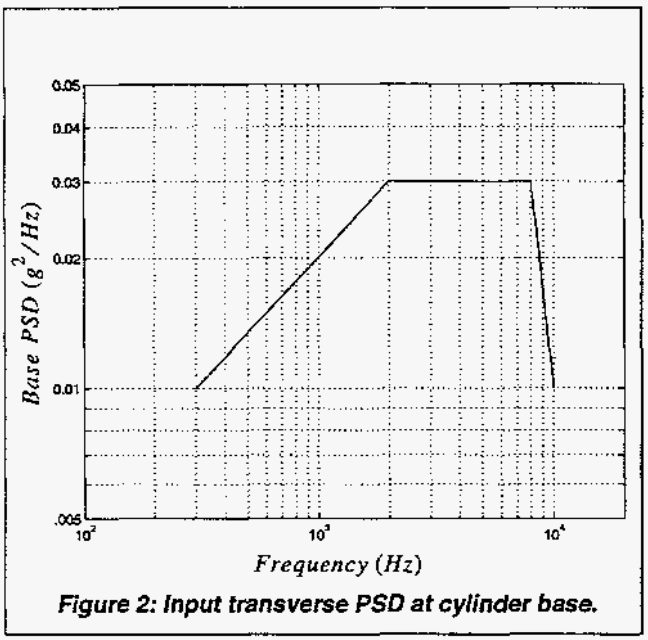

Figure 2: Input transverse PSD at cylinder base.

assume single-DOF response of the structure, choosing a single mode (typically the one with highest modal effective mass [4] within the bandwidth of the input) to compute an "equivalent static g-field" using Miles' relation. Response contributions from other structural modes are ignored. To the extent that single-DOF behavior is not realized, this method is inaccurate for ascertaining the global random stress response. A method is proposed here that accurately captures the RMS von Mises stress from all excited modes throughout the structure, and for all frequencies of interest.

3. STRUCTURE AND INPUTS

Consider a structure, *S*, for which a complete linear dynamics analysis has been performed. Input to the linear system are histories of an extended force vector

$$f = \{f_1^1(t), f_2^1(t), f_3^1(t), f_1^2(t), f_2^2(t), f_3^2(t), \ldots.\}^T, \qquad (1)$$

where the subscripts denote coordinate direction, the superscripts denote location, and $(\ )^T$ denotes the matrix transpose. The complete dynamic analysis asserted above includes generation of deterministic transfer functions mapping the imposed forces to stresses at the locations of interest.

At a location x, the stress, $\sigma(t)$, is expressed as a convolution of the imposed force history with the stress impulse response function [5],

$$\sigma = h_\sigma * f \qquad (2)$$

Computationally, and for the sake of convenience in nomenclature, σ is taken to be an algebraic vector of length six, $[\sigma_{xx}, \sigma_{yy}, \sigma_{zz}, \sigma_{xy}, \sigma_{xz}, \sigma_{yz}]$ consisting of the non-redundant components of the stress tensor. Representing the number of rows of f as N_F, the impulse response function h_σ is a $6xN_F$ matrix.

The common use of digitized data and the Fast Fourier Transform (FFT) suggest a restatement of the above equations in terms of Fourier series. Further, the linear analysis is conveniently and conventionally expressed in terms of transfer functions in the frequency domain.

Let the force vector be expressed as,

$$f(t) = \sum_{n=1}^{N_\omega} Re\{\hat{f}_n e^{in\zeta}\}, \qquad (3)$$

where $\zeta = 2\pi t/T$, T is a period on the order of the time of the experiment, and $\hat{f}_n$ is the n^{th} frequency component of f. Here it is assumed that the time-averaged value of the imposed force is zero.

The frequency domain representation of f is given by,

$$\hat{f}_n = \frac{2}{T}\int_0^T f(t) e^{-2\pi i n t/T} dt \qquad (4)$$

In general, f is known only in a statistical sense, and its transform $\hat{f}$ is known to the same extent.

When Eq. (3) is substituted into Eq. (2), we find,

$$\sigma(t) = \sum_{n=1}^{N_\omega} Re\{\hat{\sigma}_n e^{in\zeta}\}, \qquad (5)$$

where

$$\hat{\sigma}_n = H_{\sigma,n}\hat{f}_n \qquad (6)$$

and

$$H_{\sigma,n} = \int_0^\infty h_\sigma(s) e^{-2\pi i n s/T} ds. \qquad (7)$$

The input is often specified in terms of a cross spectral density matrix given by

$$S_F(n) = \frac{T}{2} E[\overline{\hat{f}_n}\hat{f}_n^T] \qquad (8)$$

where $E[\ ]$ is the expected value obtained by ensemble averaging [6] and $\overline{(\ )}$ is the complex conjugate operator.

For a single force input, this is the autospectral density,

$$s_F(n) = \frac{T}{2} E[|f_n|^2]. \qquad (9)$$

4. RMS VON MISES STRESS IN FREQUENCY DOMAIN

It is of interest to calculate the mean value of the square of the von Mises stress over a given time period. (In fact, the

method presented here can be used to examine any other quadratic functions of the linear output variables.) The quadratic functions of the output variables, such as squared von Mises stress, must be mapped from the imposed force.

Consider quadratic functions of stress, written in the following form,

$$p(t)^2 = \sigma^T A \sigma \tag{10}$$

where A is a symmetric, constant, positive semi-definite matrix. In the case of von Mises stress,

$$p(t)^2 = \sigma_{xx}^2 + \sigma_{yy}^2 + \sigma_{zz}^2 - (\sigma_{xx}\sigma_{yy} + \sigma_{xx}\sigma_{zz} + \sigma_{yy}\sigma_{zz}) + 3(\sigma_{xy}^2 + \sigma_{xz}^2 + \sigma_{yz}^2)$$

and,

$$A = \begin{bmatrix} 1 & -\frac{1}{2} & -\frac{1}{2} & & & \\ -\frac{1}{2} & 1 & -\frac{1}{2} & & & \\ -\frac{1}{2} & -\frac{1}{2} & 1 & & & \\ & & & 3 & & \\ & & & & 3 & \\ & & & & & 3 \end{bmatrix} \tag{11}$$

Equation (10) expanded in Fourier terms is

$$p^2 = \sum_{m=1}^{N_\omega} Re\{\hat{\sigma}_m^T e^{im\zeta}\} A \sum_{n=1}^{N_\omega} Re\{\hat{\sigma}_n e^{in\zeta}\}, \tag{12}$$

and some trigonometric manipulations show the time-averaged value of the square of von Mises stress to be

$$\langle p^2 \rangle = \frac{1}{2} \sum_{n=1}^{N_\omega} [\hat{\sigma}_n^\dagger A \hat{\sigma}_n] \tag{13}$$

where $(\ )^\dagger$ denotes the Hermitian operator (complex conjugate transpose).

Equation (13) is a form of Parseval's theorem [7]. The root-mean-square value, p_{RMS}, of p is given by

$$p_{RMS} = \sqrt{\langle p^2 \rangle}. \tag{14}$$

To be useful, the above expansions must be expressed in terms of the input forces

$$\langle p^2 \rangle = \frac{1}{2} \sum_{n=1}^{N_\omega} \hat{f}_n{}^\dagger H_{\sigma,n}^\dagger A H_{\sigma,n} \hat{f}_n. \tag{15}$$

With ensemble averaging, Eq. (15) can be expressed in terms of the input cross spectral density matrix of Eq. (8).

$$\langle p^2 \rangle = \frac{1}{T} \sum_{n=1}^{N_\omega} \sum_{i,j=1}^{N_F} (H_{\sigma,n}^\dagger A H_{\sigma,n})_{i,j} \, S_F(n)_{i,j}. \tag{16}$$

The one-dimensional version of Eq. (16) has been used previously in stress analysis [3,8], but the equations presented here appear to be the first that accommodate the full stress tensor.

5. RMS STRESS USING MODAL SUPERPOSITION

Modal superposition provides a convenient framework for computation of RMS stress invariants. The linear components of the stress (not principal stresses) can be superposed since they are derivatives of linear functions. Let $\Psi_{\sigma,i}^b$ represent the stress components (1 to 6) for mode i, evaluated at node b. The "stress modes" are standard output from most FEA modal analysis codes (such as the grid point stresses in MSC/NASTRAN [9]).

The transfer function for a stress at location b due to an input force at degree of freedom a, can be written as [10]

$$H_{\sigma,n}^{ab} = \sum_{i}^{\#\,\text{modes}} \frac{\Psi_{\sigma,i}^b \varphi_{ai}}{\omega_i^2 - \omega_n^2 + 2j\gamma_i\omega_n} = \sum_i \Psi_{\sigma,i}^b \varphi_{ai} D_i(n). \tag{17}$$

Here, φ is the displacement eigenvector, and D contains all frequency dependence. For a single axis shaker, Eqs. (16) and (17) can be combined to give

$$\langle p^2 \rangle = \frac{1}{T} \sum_n \sum_{i,j} \Psi_{\sigma,i}^b \varphi_{ai} D_i^\dagger(n) A \Psi_{\sigma,j}^b \varphi_{aj} D_j(n) s_F(n). \tag{18}$$

Grouping terms and simplifying,

$$\langle p^2 \rangle = \sum_{i,j}^{\#\,\text{modes}} Q_{ij} T_{ij} R_{ij}, \tag{19}$$

where

$$Q_{ij} = \varphi_{ai}\varphi_{aj} \tag{20}$$

$$T_{ij} = \Psi_{\sigma,i}^b A \Psi_{\sigma,j}^b \quad \text{and} \tag{21}$$

$$R_{ij} = \frac{1}{T} \sum_n D_i^\dagger(n) D_j(n) s_F(n). \tag{22}$$

Here, Q_{ij} depends only on the shaker input location, T_{ij} depends only on the node location for stress output, and R_{ij} contains all the frequency dependence of the problem.

To obtain results at every node, Q and R may be evaluated only once while T and the modal sums must be computed at

each node. Computation of R is of order N_ω. Within a modal survey, the total computation is of order M^2N where M is the number of modes, and N is the number of nodes in the survey. Even for a very large model, these computations are easily accomplished on a workstation.

The same approach can be extended to problems with multiple input forces by adding dimensionality to Q and R.

6. RESULTS AND VERIFICATION

The shell elements used to model the cylinder in Fig. 1 produce no out-of-plane stresses [9]. Therefore, in element coordinates, the three remaining nonzero stress components are σ_x, σ_y (normal stress) and τ_{xy} (shear stress). In this context, A reduces to a 3 x 3 matrix,

$$A = \begin{bmatrix} 1 & -\frac{1}{2} & \\ -\frac{1}{2} & 1 & \\ & & 3 \end{bmatrix} \qquad (23)$$

The transfer functions for the stress components were computed from Eq. (17) at each grid point in the model. A typical set of transfer functions at one of the grid points is illustrated in Fig. 3. The stress and displacement eigenvectors, Ψ and φ, required to compute the transfer functions were obtained using MSC/NASTRAN, and 1% modal damping was applied.

The mean squared von Mises stresses at each grid point were calculated using three methods: (a) time realization using Eq. (10) and an inverse FFT of Eq. (6); (b) direct frequency realization of Eq. (13) using Eq. (16); and (c) the implementation of Eq. (13) using the efficient modal superposition procedure of Eq. (19). The mean squared von Mises stresses at each grid point were found to be identical using each of the three methods, thus verifying the procedure.

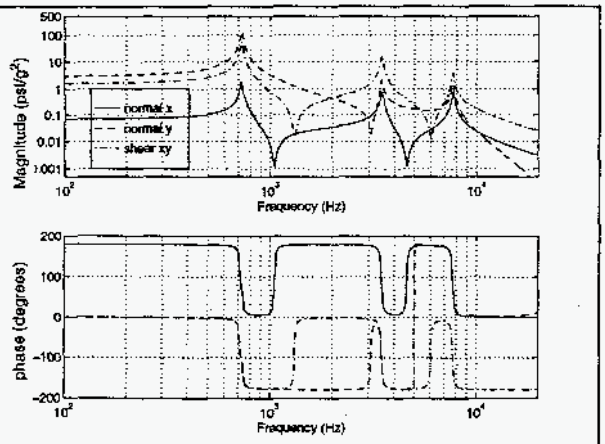

Figure 3: Stress component transfer functions.

Time and frequency realizations of the input acceleration and output stresses at a typical point are shown in Figs. 4 and 5, respectively. Time and frequency plots for the mean squared and RMS von Mises stresses at the same location are presented in Fig. 6. The RMS von Mises stresses at all grid points were computed from Eqs. (14) and (19), with contours of this quantity plotted in Fig. 7.

As illustrated in Fig. 5, the shear and one of the normal stress components dominate the stress state at this location. σ_y is driven by the first bending mode of the cylinder, at 724 Hz. τ_{xy} is driven by both first and second bending modes, the second

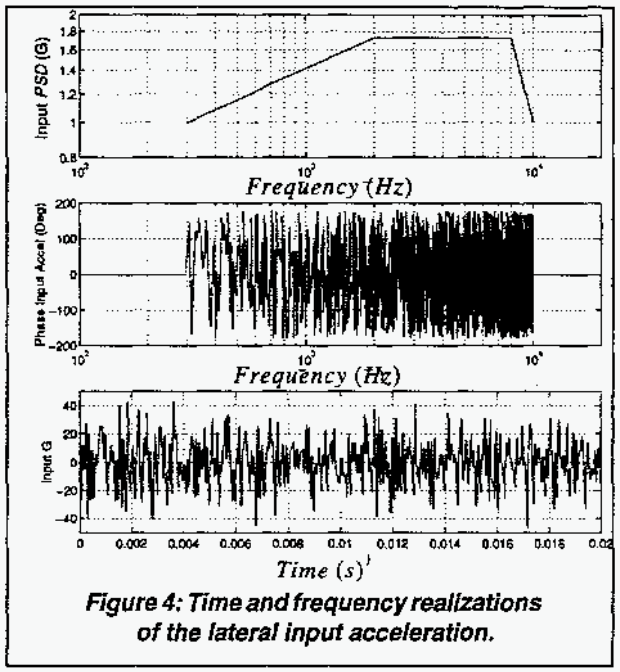

Figure 4: Time and frequency realizations of the lateral input acceleration.

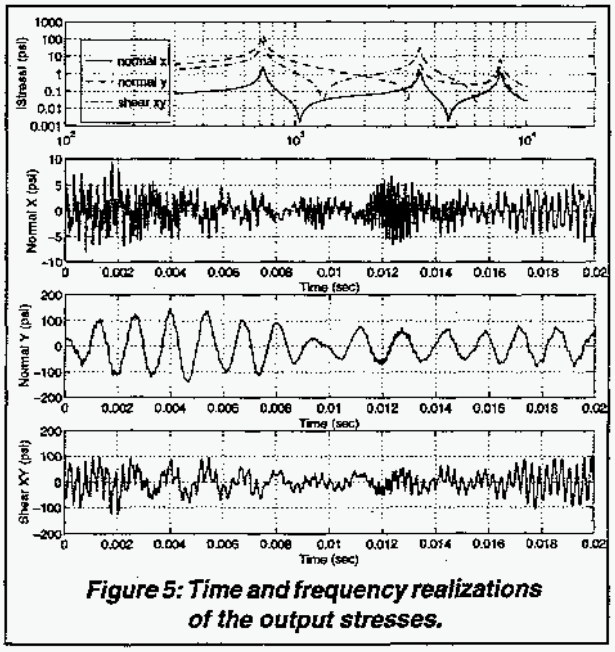

Figure 5: Time and frequency realizations of the output stresses.

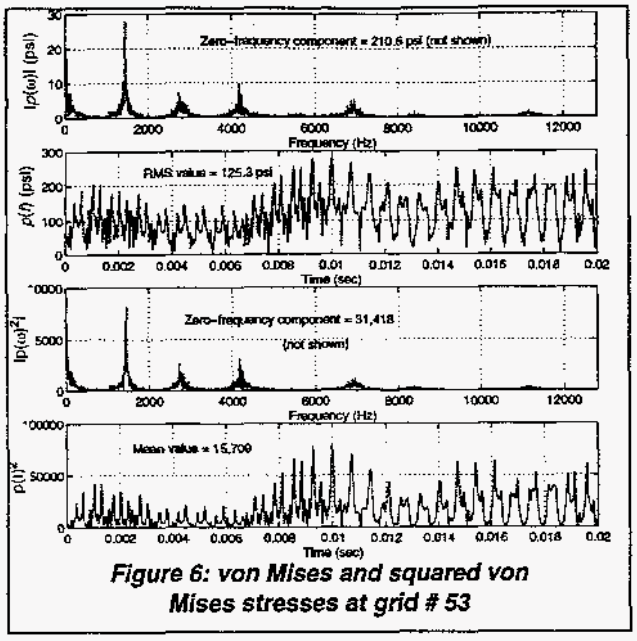

Figure 6: von Mises and squared von Mises stresses at grid # 53

occurring at 3464 Hz. The relatively low σ_x stress is driven by the first three modes, the third occurring at 7698 Hz.

We see in Fig. 6 that the frequency content of the squared von Mises stress contains terms at twice the excited natural frequencies (e.g., 1448 Hz, 6928 Hz). This observation is attributable to the fact that a squared sinusoid is another sinusoid at twice the original frequency (plus a constant). The linear stress components respond at the natural frequencies of the structure, while the squared von Mises stress responds at twice these frequencies. At this particular location, the $\sigma_x\sigma_y$ term in the expression for von Mises stress is small and

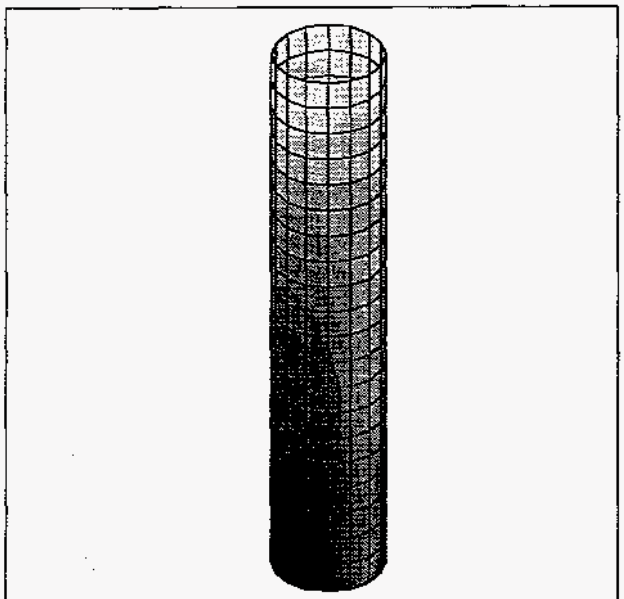

Figure 7: RMS von Mises stress contours

the first two modes, drivers for σ_y and τ_{xy}, also drive the von Mises stress. Von Mises stress frequencies also occur at $f_j - f_i$, where i,j denote excited modes. For example, Fig. 6 shows von Mises content at $f_2 - f_1 = 3464 - 724 = 2740$ Hz and at $f_3 - f_2 = 7698 - 3464 = 4234$ Hz.

7. COMPARISON WITH MILES' RELATION

Evaluations of RMS von Mises stress using the new procedure and the traditional Miles' relation were compared. A new input acceleration PSD was generated, as shown in Fig. 8. Three cases were examined in which the input PSD frequency range was selected to excite (a) only the first mode, (b) only the second mode and (c) both first and second modes. To excite the first mode only, the input PSD followed the definition of Fig. 8 up to 1000 Hz, and was set to zero beyond this frequency. For second mode response, the input PSD was set to zero below 1000 Hz and followed the Fig. 8 definition between 1000 and 10,000 Hz. Excitation of both modes resulted by applying the full PSD from zero to 10,000 Hz.

Miles' method assumes single-DOF behavior of a structure. An additional constraint on the application of Miles' relation to elastic structures is that the shape of the single excited mode must approximate the profile of the structure under a static g-field. For example, the first mode of a cantilever beam assumes the approximate shape of the beam under a transverse g-field.

Miles' relation is given by,

$$g_{eq} = \sqrt{f_m PSD(f_m) \frac{\pi}{2} Q} \qquad (24)$$

where g_{eq} is the approximate RMS acceleration response, commonly used as an "equivalent static-g field", f_m is the single natural frequency chosen for application of Miles' relation, $PSD(f_m)$ is the value of the input acceleration PSD at frequency f_m, and Q is the quality factor, defined as $1/(2\zeta)$.

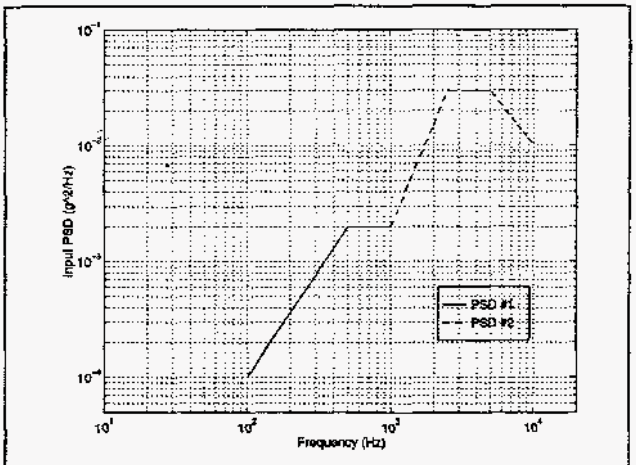

Figure 8: Input PSD for Miles' comparison

For the input PSD shown in Fig. 8, g_{eq} from Eq. (24) is 10.7 g for the first mode at 724 Hz, and 90.3 g for the second mode at 3464 Hz.

Because the von Mises stress in a static g-field scales with the magnitude of the field, the static response of the cantilevered cylinder to a 1-g field may be used to scale the Miles' approximations for each mode. The displacement and von Mises stress responses to a transverse 1-g field are presented in Figure 9. The profile of the static response is similar to the first mode of a cantilever beam. The maximum von Mises stress corresponding to the 1-g static field is 12.6 psi, and occurs at the base top and bottom-most fibers. Thus, the maximum von Mises stresses corresponding to the Miles' equivalents for the first and second modes are 134.4 and 1138.3 psi, respectively.

The true RMS von Mises stresses were computed using the new method presented above. The stress contours which result from the application of the input PSD below 1000 Hz are superimposed upon the deformed shape for the first mode in Fig. 10. The stress contours and shape profile closely resemble those of the static-g response. The maximum RMS von Mises stress for this case is 117.4 psi, showing the Mile's method to be slightly conservative.

When the second mode alone is excited by applying the input PSD above 1000 Hz, an entirely different result is obtained. The von Mises stress contours for this case are superimposed upon the deformed shape for the second mode in Fig. 11. The stress contours and shape profile do not resemble those of the static-g response. The maximum RMS von Mises stress for this case is 106.3 psi, showing the Mile's method to be conservative by an order of magnitude.

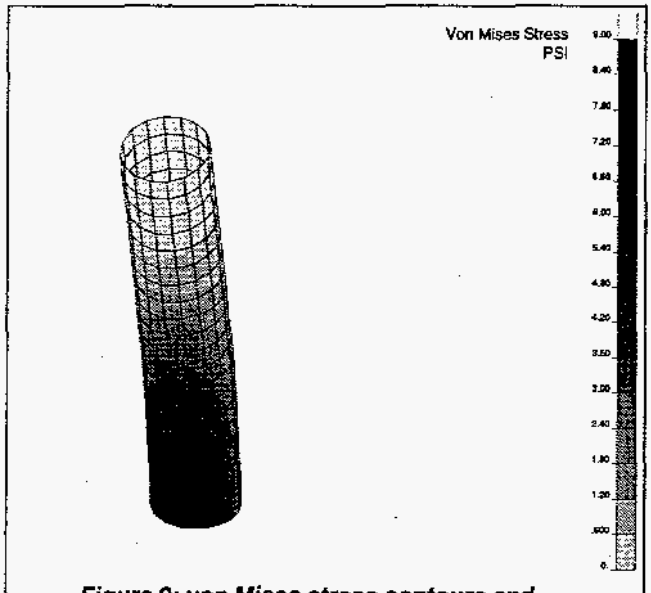

Figure 9: von Mises stress contours and displacements for a transverse 1-g field

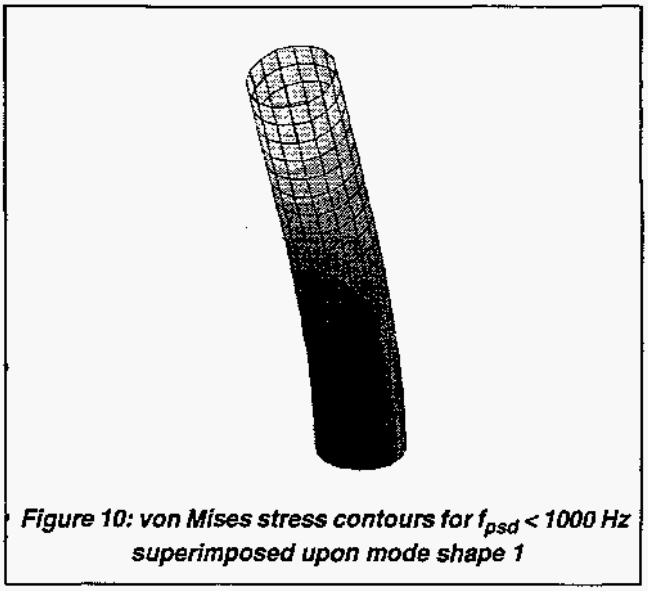

Figure 10: von Mises stress contours for f_{psd} < 1000 Hz superimposed upon mode shape 1

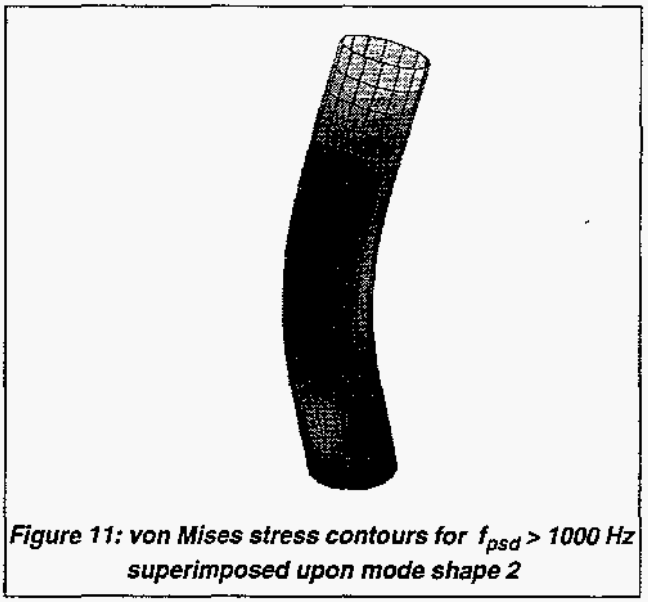

Figure 11: von Mises stress contours for f_{psd} > 1000 Hz superimposed upon mode shape 2

Finally, the entire PSD of Fig. 8 was applied to the cylinder, and the resulting von Mises stress contours are superimposed upon the first and second mode shapes in Figures 12 and 13. The contours are observed to be a blend of the two narrow-band responses, with the maximum RMS von Mises stress at 158.4 psi. The first-mode Miles' approximation is slightly non-conservative, whereas the second-mode approximation is much too conservative.

8. SUMMARY AND CONCLUSIONS

A computationally efficient method has been developed for calculating the RMS von Mises stress in a random vibration environment. The method retains the full accuracy of the FEM model and modal analysis. Surveys of the RMS stress for the entire structure can be computed efficiently. The number of operations per node output is of order M^2, where M is the

Figure 12: von Mises stress contours for $0 < f_{psd} < 10$ KHz superimposed upon mode shape 1

Figure 13: von Mises stress contours for $0 < f_{psd} < 10$ KHz superimposed upon mode shape 2

number of modes computed. Results exactly match a full time history development.

Conditions under which Miles' relation produces good estimates of von Mises stress contours were examined, as well as conditions resulting in poor estimates. Miles' relation is adequate when the system response is dominated by a single mode, and when the excited mode shape approximates the response to a static g-field. Otherwise, both conservative and non-conservative estimates may result from the application of Miles' relation.

Work underway will further quantify the statistical properties of the von Mises stress. These properties will determine the probability of the von Mises stress exceeding a given value for infinite time and finite time force histories.

9. ACKNOWLEDGEMENTS

Sandia National Laboratories is a multiprogram laboratory operated by Sandia Corporation, a Lockheed Martin Company, for the United States Department of Energy under Contract DE-AC04-94AL85000.

10. REFERENCES

[1] Shigley, Joseph E., *Mechanical Engineering Design*, 2nd ed., McGraw-Hill, NY, 1972 pp 232-236.

[2] Miles, John W. "On the Structural Fatigue under Random Loading", Journal of the Aeronautical Sciences, Nov 1954.

[3] Ferebee, R. C. and Jones, J. H. "Comparison of Miles' Relationship to the True Mean Square Value of Response for a Single Degree of Freedom System", NASA/Marshall Space Flight Center

[4] Kammer, D.C., Flanigan, C.C., and Dreyer, W., "A Superelement Approach to Test-Analysis Model Development," Proceedings of the 4th International Modal Analysis Conference, Los Angeles, CA, February, 1986.

[5] Meirovitch, L. *Elements of Vibration Analysis*, McGraw-Hill, NY, 1975, p. 68.

[6] Bendat, J. and A. Piersol, *Random Data: Analysis and Measurement Procedures*, John Wiley & Sons, NY, 1986, pp. 244-246.

[7] Rudin, W., *Real and Complex Analysis,* McGraw-Hill, New York, 1966, p. 85.

[8] Madsen, H., "Extreme-value statistics for nonlinear stress combination", *Journal of Engineering Mechanics, Vol. 111,* No. 9, Sept. 1985, pp 1121-1129.

[9] MSC/NASTRAN Quick Reference Guide, Version 68. MacNeal-Schwendler Corp.

[10] Craig, Roy R. Jr., *Structural Dynamics, An Introduction to Computer Methods*, John Wiley & Sons, NY, 1981, pp. 356, 366.

[11] Soong, T.T. and M. Grigoriu, *Random Vibration of Mechanical and Structural Systems*, Prentice-Hall, Englewood Cliffs, NJ, 1993.

[12] Thomson, William T., *Theory of Vibration with Applications*, Prentice-Hall, Englewood Cliffs, NJ, 1981.

[13] MATLAB Reference Guide, The MathWorks, Inc., 1992.